Supplement of

Light Absorption by Brown Carbon over the South-East Atlantic Ocean

Lu Zhang et al.

Correspondence to: Lu Zhang (luzhang@mail.tau.ac.il)

S1 Experimental

S1.1 Instrumentation

A High-Resolution Time-of-Flight Aerosol Mass Spectrometer (HR-ToF-AMS, Aerodyne Research, Inc.) was deployed to obtain mass concentrations of sulphate (SO_4^{2-}), nitrate (NO_3^-), ammonium (NH_4^+), chloride (Cl^-), and organic aerosol (OA) from particles with vacuum aerodynamic diameters between 50 to 500 nm.

These mass concentrations were then used to calculate the bulk refractive index based on different mixing rules. To better distinguish BB influences, the AMS fragment analysis was applied to give f44 and f60, representing the ratios of m/z 44 (CO_2^+) and m/z 60 ($C_2H_4O_2^+$), respectively, to total organic signal.

The mass and number concentrations of the refractory BC particles and the single-particle masses and mixing states were measured by the Single-Particle Soot Photometer (SP2, Droplet Measurement Technologies). Scattering by individual coated BC particles, derived using the leading-edge-only (LEO) method of Gao et al. (2007), was used to estimate rBC-containing particle coating thicknesses for use with optical models. The SP2 detects BC particles with core diameters from 80-650 nm; to account for BC particles with core diameters outside this range, a lognormal function was fit to BC number size distribution (Schwarz et al., 2006). The diameter of BC as mass equivalent diameter was calculated as $(6m/\rho\pi)^{1/3}$, where m represents the mass of the BC particle and ρ represents the density of BC, assumed to be 1.8 g cm^{-3} (Bond and Bergstrom, 2006). The uncertainty of the measured BC mass concentration is estimated to be ±17% (Laborde et al., 2012).

The Ultra-High-Sensitivity Aerosol Spectrometer (UHSAS, Droplet Measurement Technologies) measured optical diameters of aerosol particles from 60 to 1000 nm; it is assumed that these optical diameters are the same as the volume equivalent diameters. UHSAS is found to have under-sizing issues according to Howell et al. (2021). We employed the empirical correction equation proposed by Howell et al. (2021) to correct UHSAS data for all legs; results will be discussed in detail in the following section.

An Aerodynamic Particle Sizer (APS, Model 3321, TSI, Inc., USA) was employed to measure the particle number size distribution (PNSD) for aerodynamic diameters between 500 nm and 20 μm. The aerodynamic diameters measured by APS were converted to volume equivalent diameters according to DeCarlo et al. (2004) under the assumption that the particles were spherical and had a density of 1.5 g cm^{-3}. Number size distributions measured by UHSAS and APS were then combined to yield a continuous PNSD ranging from ~90 nm to 10 μm in volume equivalent diameter.

An integrating Nephelometer (Neph, TSI Inc., model 3563) was used to measure aerosol scattering coefficients at wavelengths 450, 550, and 700 nm, which were corrected for truncation based on Anderson and Ogren (1998). The instrument was operated at ambient relative humidity (RH), so the particles were not necessarily dry, especially for those within the planetary boundary layer (PBL). The uncertainty of the scattering coefficients measured by Neph is ~10%.

A Particle Soot Absorption Photometer (PSAP, Radiance Research) was used to determine aerosol absorption coefficients at wavelengths 470, 530, and 660 nm, which were corrected with the wavelength-average Virkkula

correction (Virkkula, 2010) and smoothed to 10 s to reduce noise. The PSAP optical block was heated to 30°C to dry particles below their deliquescence values.

Particles were sampled on various filters, where in this analysis we refer to the results obtained by particles deposited on Paella TEM grids (for offline single particle analysis of mixing state, Dang et al., 2021), and on Teflon filters, which were used to extract soluble BrC fraction at 370 nm. For the single particle analysis, a JEOL™ JEM-2010F FEG-TEM with a ThermoNoran™ EDX detector was used to analyze the 7 filters. Around 50 particles were analyzed per filter. TEM was performed at 200 KeV accelerating voltage, with a take-off angle of 15.9 degrees for X-ray emission from the sample. The elemental weight percentage per particle was determined using the NSS software with the software's Cliff-Lorimer w/o Absorbance correction method.

S1.2 Verification of corrected UHSAS data

A correction for undersizing by UHSAS reported in ORACLES by Howell et al. (2021) was applied. In this section, we evaluate the corrected PNSD by comparing calculated and measured scattering coefficients at their native measured wavelengths of 450, 550, and 700 nm. We used all four models to calculate the scattering coefficients with m_{BC} (refractive index of BC) of 1.95+0.79i and m_{OA} (refractive index of OA) of 1.65+0i.

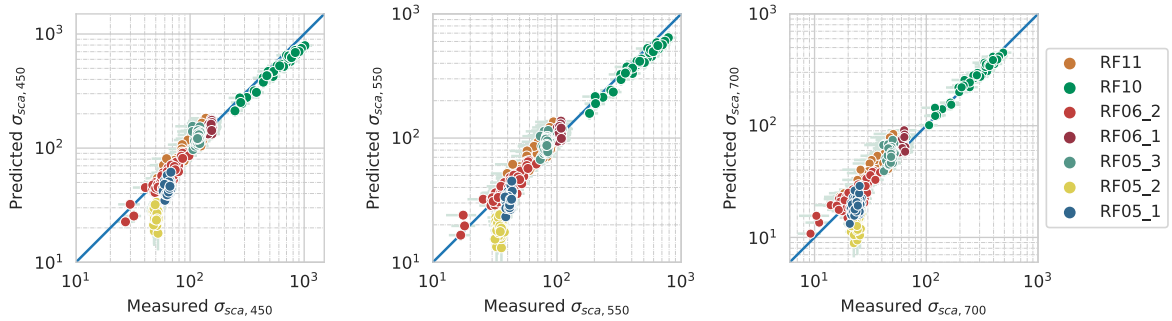

Figure S1: Measured and calculated scattering coefficients σ_{sca} at 450, 550, 700 nm for all samples. Scattering coefficients are calculated with the corrected UHSAS data using CS model assuming non-absorbing OA. Indices of refraction for BC and OA, m_{BC} and m_{OA}, were taken as 1.95+0.79i and 1.65+0i, respectively. Colours represent different filters.

Figure S1 shows the comparison of measured and calculated scattering coefficients with corrected UHSAS data for each sample using the CS model at wavelengths 450, 550, and 700 nm. Only results from CS model are presented, as similar results were obtained for the other three models. Generally, except for samples from RF05_1 and RF05_2, the correction equation worked well and there was good agreement between measured and predicted scattering coefficients at all three wavelengths. However, for samples taken from RF05_1 and RF05_2, the calculated scattering coefficients underestimated the measurements, likely due to the difference in relative humidity (RH) between the measured and calculated scattering coefficients; the RH of the Neph was not controlled during measurements. Measurements for RF05_1 was in mixed cloud and aerosol layer and RF05_2 were taken within the marine boundary layer (MBL), where the RHs are generally higher than in other layers. The RH values inside the Neph for these two samples were 57±2% and 72±2%, respectively. Therefore, the scattering coefficients predicted under dry conditions, as shown in Fig. S1, are smaller than the measurements. In contrast, the rest of the samples were collected in the free troposphere (FT), where the RH is generally <40% and hence can be regarded as dry (Carrico et al., 2005; Zhang et al., 2015). Good agreement between calculated values and measurements was obtained by these other samples, with differences <3%, indicating that the correction worked well.

S2 Optical models used in this study

Four different optical models are used in this study: the core-shell (CS) Mie model and three homogeneous grey sphere models – the volume mixing (VM) model, Maxwell-Garnett (MG) model, and Bruggemann (BG) model.

i) The core-shell (CS) model assumes the BC core is concentrically located inside non-BC materials, i.e. the shell. Inputs of the CS model are the refractive indices of both the core and shell and the 2-D BC size and mixing state (i.e., coating thickness) distribution.

ii) For the homogeneous grey sphere models, inputs are the PNSD and effective refractive index. The three mixing rules that were used to compute the effective refractive index ($m_{\text{eff}} = n+ki$) are:

   a) The volume mixing (VM) rule, which assumes components are well mixed within the particle. Similar to the calculation of bulk density, the effective refractive index (m_{eff}) is calculated following the volume mixing rule:

$$m_{eff} = \sum_i f_i m_i \tag{1}$$

   where f_i is the volume fraction of component i, and m_i is the refractive index of component i.

   b) The Maxwell-Garnett (MG) mixing rule assumes an inclusion (BC in our case) with permittivity ε_1 and volume fraction f_1 is embedded within a host medium (non-BC materials) with permittivity ε_2. The effective permittivity can be computed as (Bohren and Huffman, 2008):

$$\epsilon = \frac{\epsilon_1 + 2\epsilon_2 + 3f_1(\epsilon_1 - \epsilon_1)}{\epsilon_1 + 2\epsilon_2 - f_1(\epsilon_1 - \epsilon_2)} \tag{2}$$

   The refractive index is the square root of the permittivity:

$$m = \sqrt{\epsilon} \tag{3}$$

   c) The Bruggemann (BG) mixing rule is derived from the same base equation as the Maxwell-Garnett mixing rule, while using a different approximation. It assumes two inclusions embedded within a host matrix with a permittivity (Markel, 2016):

$$\epsilon = \frac{1}{4}(b + \sqrt{8\epsilon_1\epsilon_2 + b^2}) \tag{4}$$

$$b = 3f_1(\epsilon_1 - \epsilon_2) + 2\epsilon_2 - \epsilon_1 \tag{5}$$

   It treats the two components more symmetrically.

For BC-containing particles, f_1 represents the volume fraction of BC, which can be calculated from BC 2-D size and mixing state distributions determined by the SP2.

S3 Calculate scattering coefficients to PSAP wavelengths

The scattering Ångström exponent (SAE) was used to convert scattering coefficients measured by the Neph (at wavelengths 450, 550, and 700 nm) to those wavelengths at which the PSAP measures absorption coefficients (470, 530, and 660 nm). The SAE is defined as:

$$\text{SAE} = -\frac{\ln(\sigma_{sca,\lambda_1}/\sigma_{sca,\lambda_2})}{\ln(\lambda_1/\lambda_2)} \tag{6}$$

where λ_1 and λ_2 are the two wavelengths at which the scattering coefficient σ_{sca} is measured. Figure S2 shows an example of the results of measured scattering and absorption coefficients and scattering coefficients converted to the wavelengths matching those of the PSAP for sample RF11.

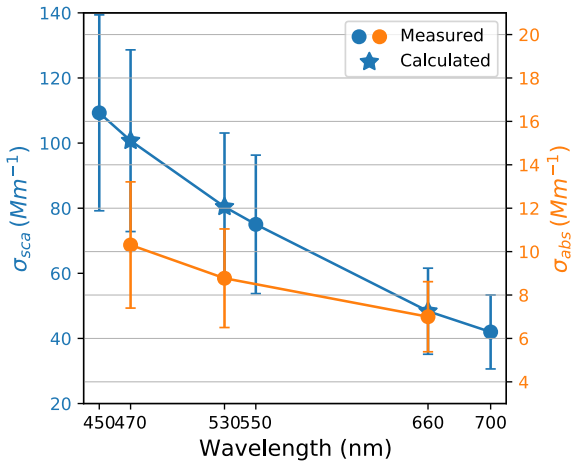

Figure S2: Measured and calculated scattering and absorption coefficients at different wavelengths. Blue and orange circles represent measured scattering coefficients σ_{sca} at 450, 550, and 700 nm from Neph and absorption coefficients σ_{abs} at 470, 530, and 660 nm from PSAP. Blue stars represent scattering coefficients interpolated with SAE of the nearest two wavelengths. This is an example for filter RF11.

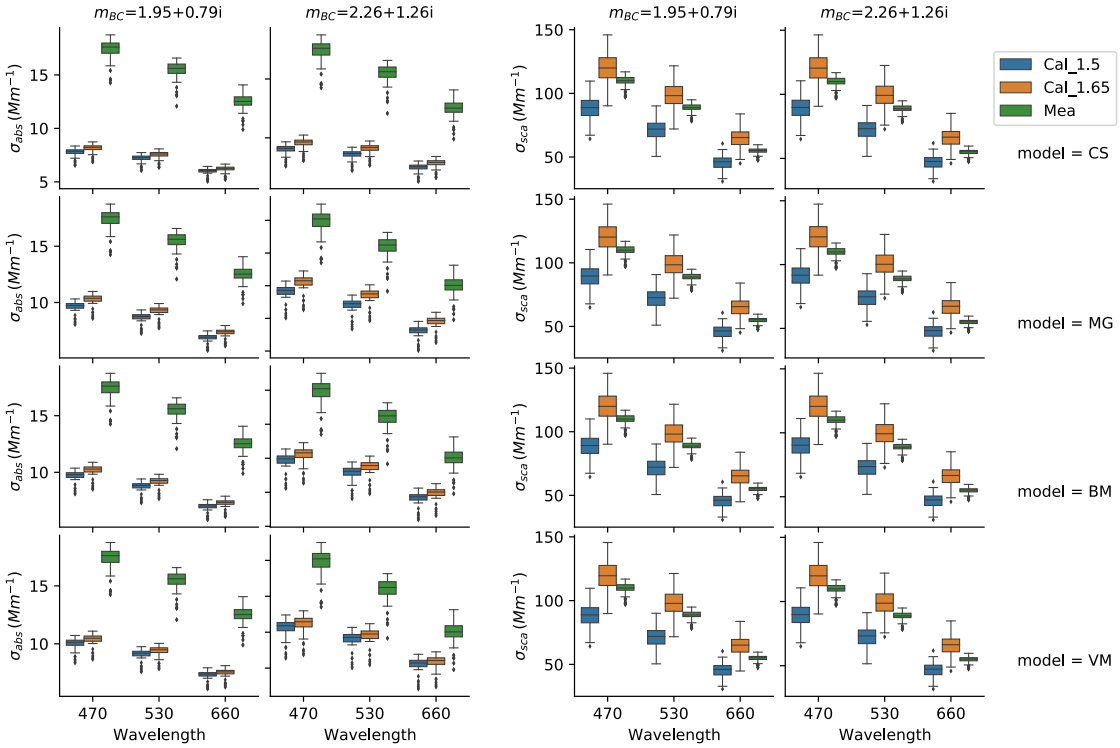

Figure S3: Modelled and measured (green markers) scattering coefficients σ_{sca} and absorption coefficients σ_{abs} at PSAP wavelengths for RF05_3. Variables are modelled with two commonly used values of m_{BC} (titled on the top) and two values of m_{OA} by the CS, MG, BG, and VM models (specified on the right). OA is assumed to be non-absorbing with indices of refraction m_{OA} equal to 1.5+0i (blue markers) and 1.65+0i (orange markers), respectively. Values of σ_{sca} measured by the nephelometer at 450, 550, and 700 nm are interpolated to PSAP wavelengths, 470, 530, and 660 nm, using the scattering Ångström exponent.

References

Anderson, T. L. and Ogren, J. A.: Determining Aerosol Radiative Properties Using the TSI 3563 Integrating Nephelometer, Aerosol Sci. Technol., 29, 57–69, https://doi.org/10.1080/02786829808965551, 1998.

Bohren, C. F. and Huffman, D. R.: Absorption and Scattering of Light by Small Particles, John Wiley & Sons, 547 pp., 2008.

Carrico, C. M., Kreidenweis, S. M., Malm, W. C., Day, D. E., Lee, T., Carrillo, J., McMeeking, G. R., and Collett, J. L.: Hygroscopic growth behavior of a carbon-dominated aerosol in Yosemite National Park, Atmos. Environ., 39, 1393–1404, https://doi.org/10.1016/j.atmosenv.2004.11.029, 2005.

Dang, C., Segal-Rozenhaimer, M., Che, H., Zhang, L., Formenti, P., Taylor, J., Dobracki, A., Purdue, S., Wong, P.-S., Nenes, A., Sedlacek, A., Coe, H., Redemann, J., Zuidema, P., and Haywood, J.: Biomass burning and marine aerosol processing over the southeast Atlantic Ocean: A TEM single particle analysis, Atmospheric Chem. Phys. Discuss., 1–30, https://doi.org/10.5194/acp-2021-724, 2021.

DeCarlo, P. F., Slowik, J. G., Worsnop, D. R., Davidovits, P., and Jimenez, J. L.: Particle Morphology and Density Characterization by Combined Mobility and Aerodynamic Diameter Measurements. Part 1: Theory, Aerosol Sci. Technol., 38, 1185–1205, https://doi.org/10.1080/027868290903907, 2004.

Howell, S. G., Freitag, S., Dobracki, A., Smirnow, N., and Sedlacek III, A. J.: Undersizing of aged African biomass burning aerosol by an ultra-high-sensitivity aerosol spectrometer, Atmospheric Meas. Tech., 14, 7381–7404, https://doi.org/10.5194/amt-14-7381-2021, 2021.

Markel, V. A.: Introduction to the Maxwell Garnett approximation: tutorial, JOSA A, 33, 1244–1256, https://doi.org/10.1364/JOSAA.33.001244, 2016.

Schwarz, J. P., Gao, R. S., Fahey, D. W., Thomson, D. S., Watts, L. A., Wilson, J. C., Reeves, J. M., Darbeheshti, M., Baumgardner, D. G., Kok, G. L., Chung, S. H., Schulz, M., Hendricks, J., Lauer, A., Kärcher, B., Slowik, J. G., Rosenlof, K. H., Thompson, T. L., Langford, A. O., Loewenstein, M., and Aikin, K. C.: Single-particle measurements of midlatitude black carbon and light-scattering aerosols from the boundary layer to the lower stratosphere, J. Geophys. Res. Atmospheres, 111, https://doi.org/10.1029/2006JD007076, 2006.

Virkkula, A.: Correction of the Calibration of the 3-wavelength Particle Soot Absorption Photometer (3λ PSAP), Aerosol Sci. Technol., 44, 706–712, https://doi.org/10.1080/02786826.2010.482110, 2010.

Zhang, L., Sun, J. Y., Shen, X. J., Zhang, Y. M., Che, H., Ma, Q. L., Zhang, Y. W., Zhang, X. Y., and Ogren, J. A.: Observations of relative humidity effects on aerosol light scattering in the Yangtze River Delta of China, Atmospheric Chem. Phys., 15, 8439–8454, https://doi.org/10.5194/acp-15-8439-2015, 2015.